Electronic supplementary information (ESI)

Polarization of Tumor-Associated Macrophages Phenotype via Hollow Iron Nanoparticles for Tumor Immunotherapy *in vivo*

Ke Li, Lu Lu, Chencheng Xue, Ju Liu, Ye He, Jun Zhou, Zengzilu Xia, Liangliang Dai*, Zhong Luo*, Yulan Mao, Kaiyong Cai*

Key Laboratory of Biorheological Science and Technology, Ministry of Education, College of Bioengineering, Chongqing University, Chongqing 400044, PR China.

E-mail: dailiangliangnbe@sina.cn; luozhong918@cqu.edu.cn; kaiyong_cai@cqu.edu.cn

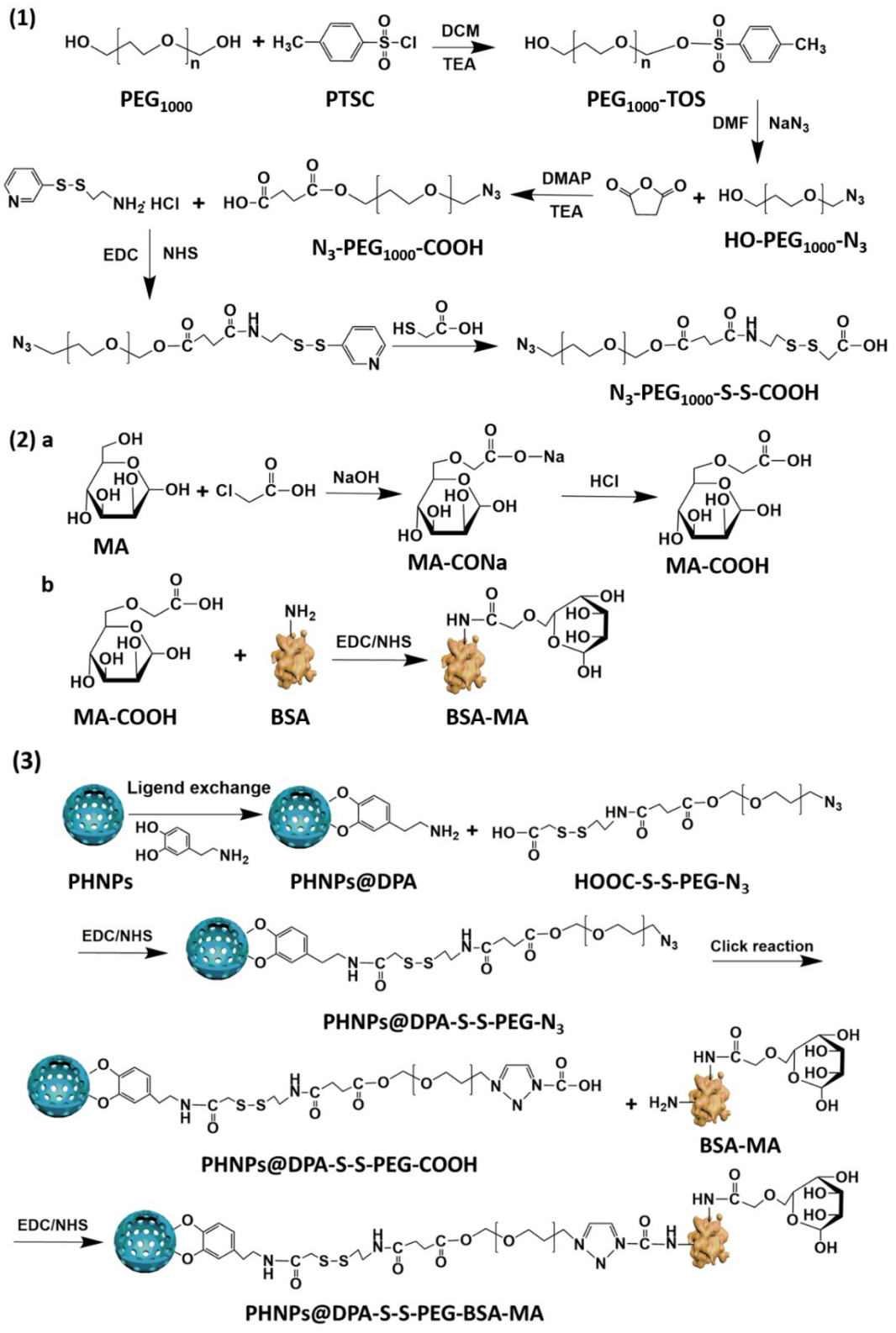

Scheme S1. The synthesis of route diagram of (1) N_3-PEG-S-S-COOH; (2, a) MA-COOH; (2, b) BSA-MA; and (3) PHNPs@DPA-S-S-PEG-BSA-MA, respectively.

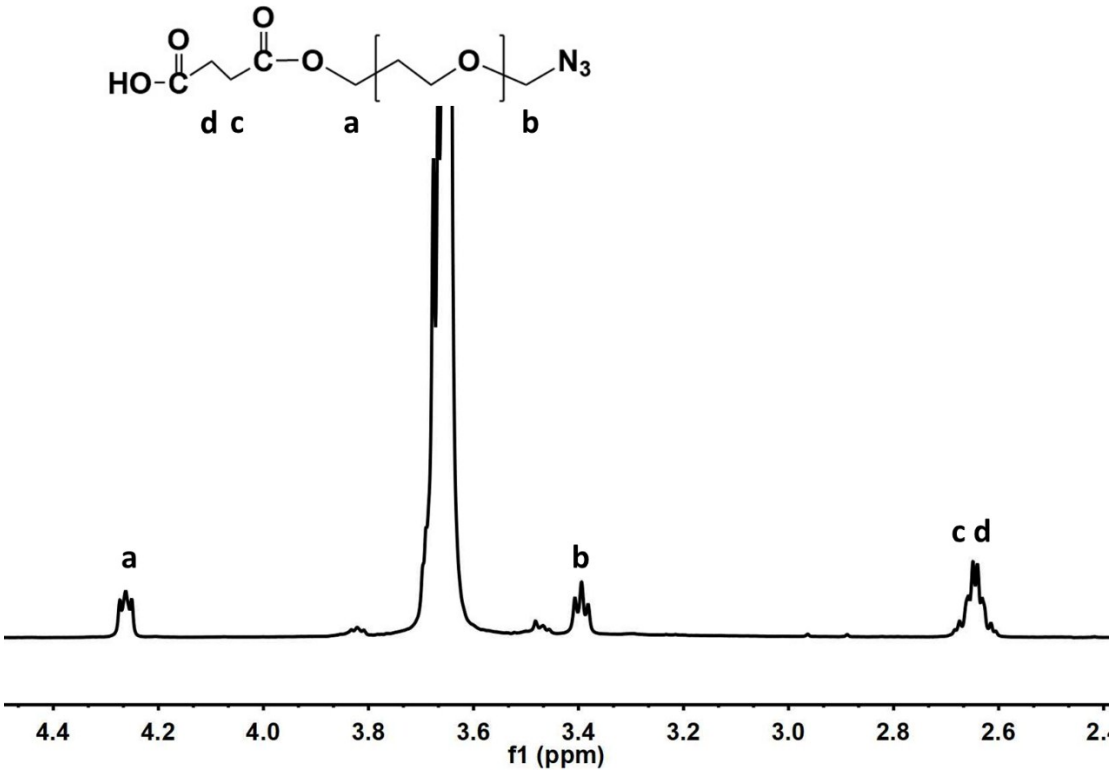

Fig. S1. ^{1}H NMR spectra of N_3-PEG-COOH

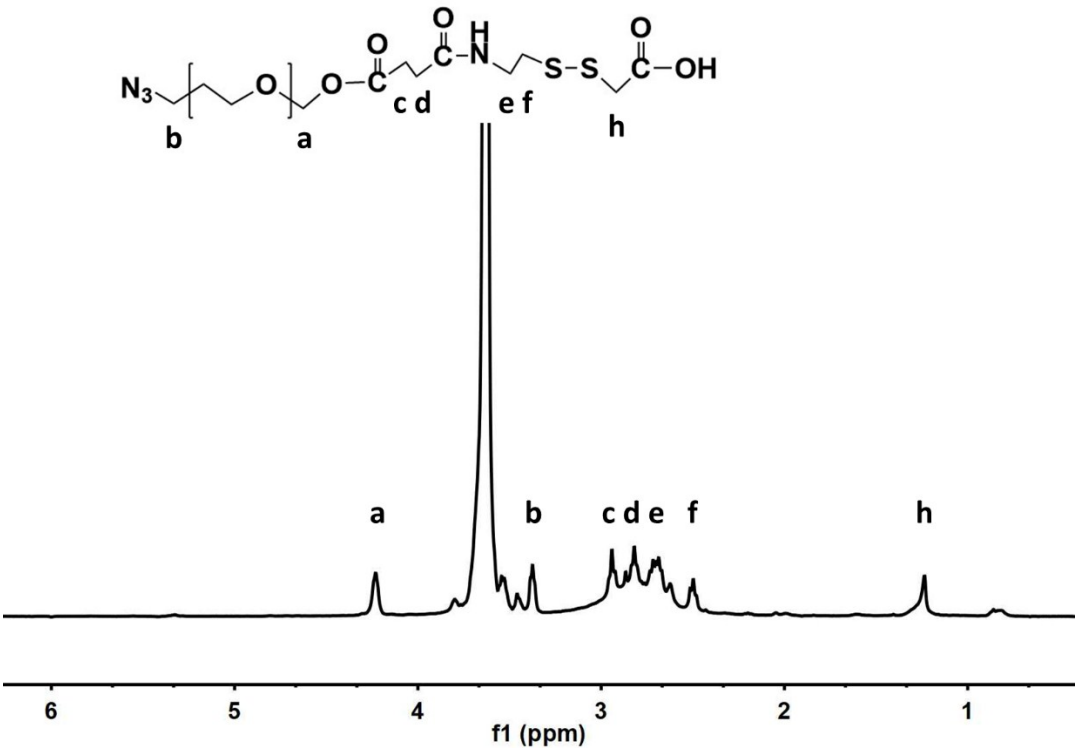

Fig. S2. ^{1}H NMR spectra of N_3-PEG-S-S-COOH

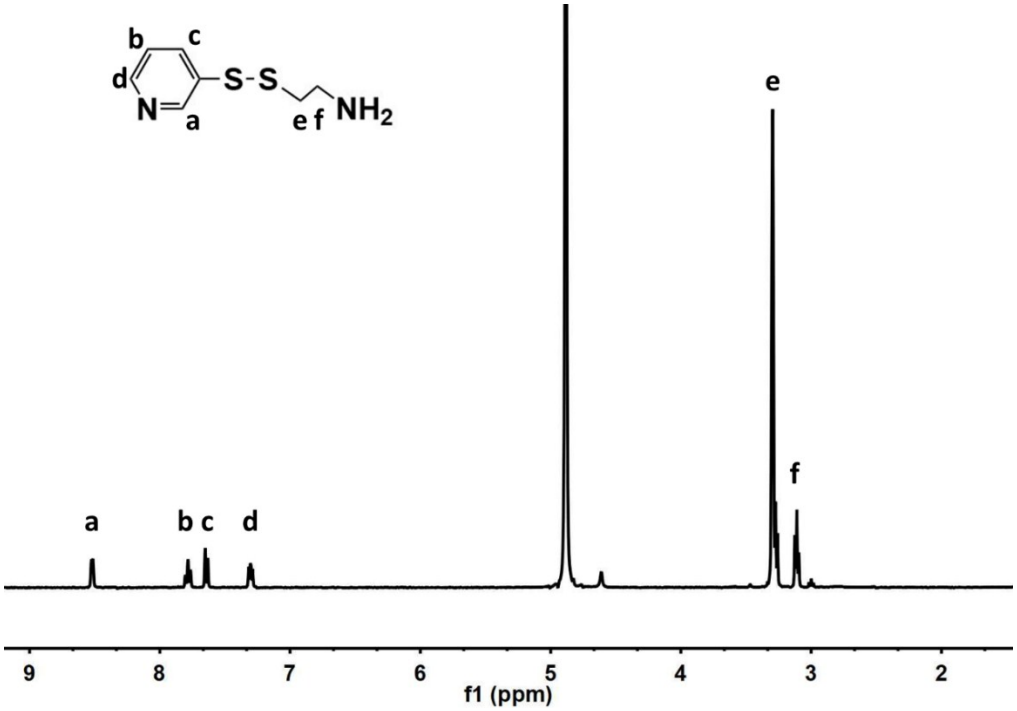

Fig. S3. ^{1}H NMR spectra of s-(2-aminoethylthio)-2-thiopyridine hydrochloride.

a

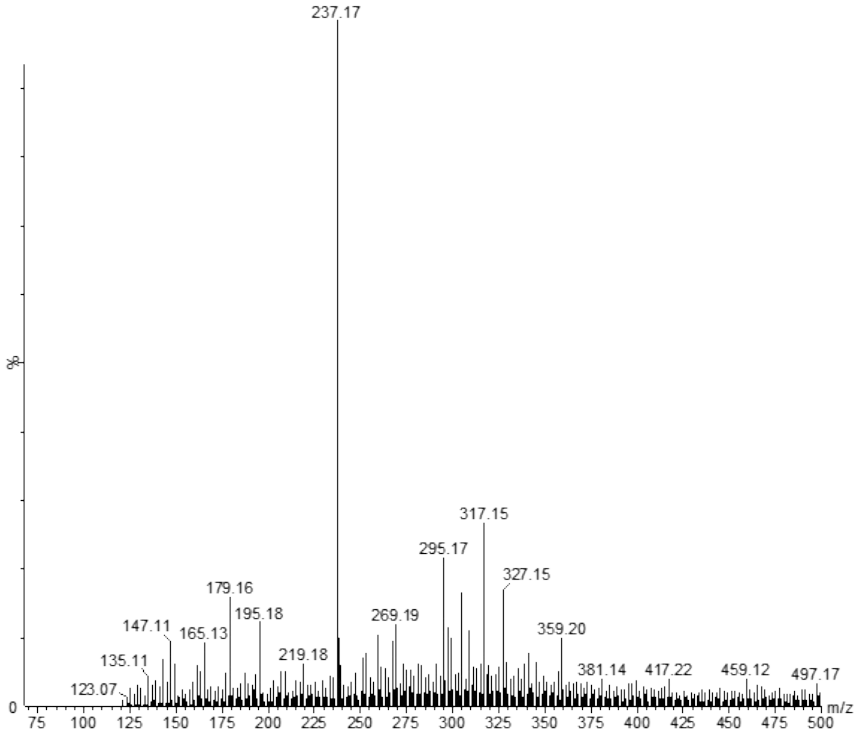

b

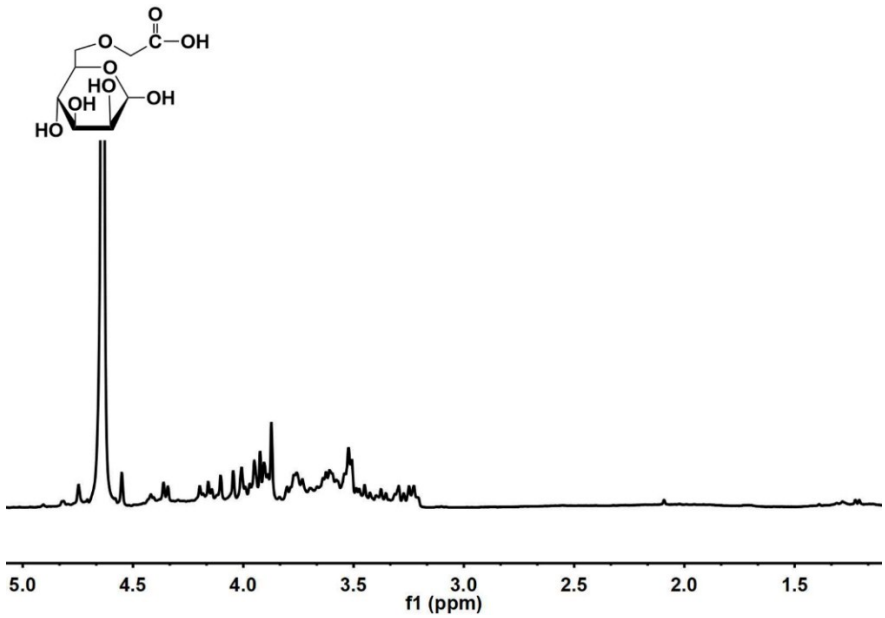

Fig. S4. HPLC analysis (a) and ^{1}H NMR spectra (b) of MA-COOH.

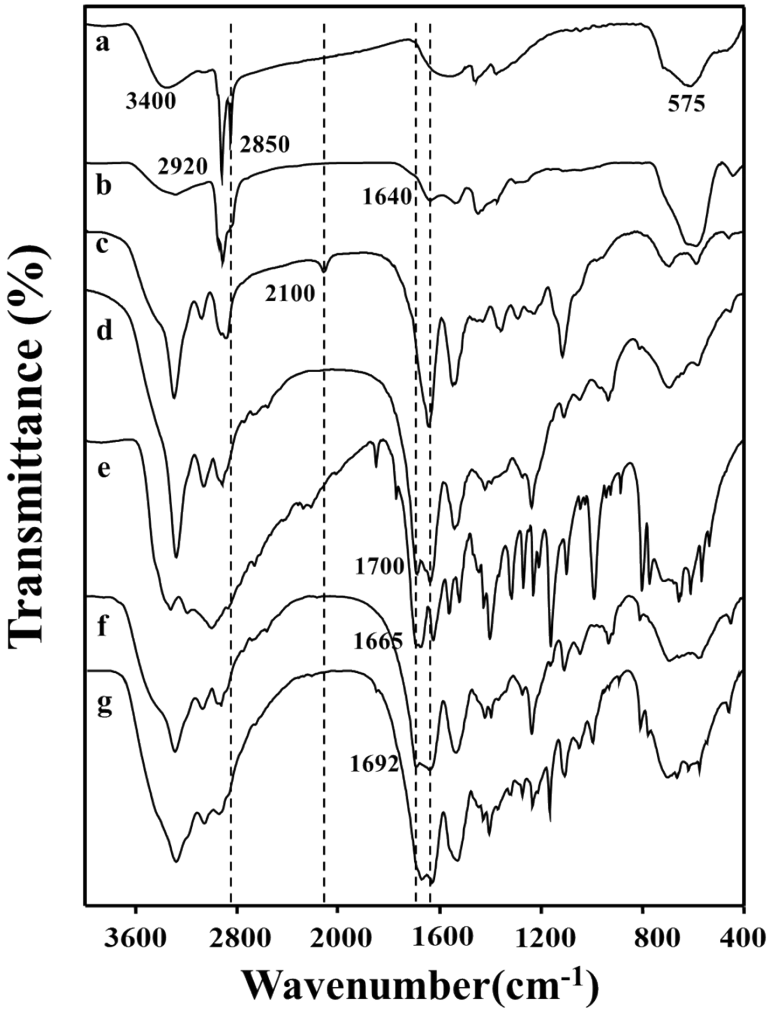

Fig. S5. FITR spectra of (a) PHNPs, (b) PHNPs@DPA, (c) PHNPs@DPA-S-S-PEG-N3, (d) PHNPs@DPA-S-S-PEG-COOH, (e) 3-MA, (f) PHNPs@DPA-S-S-PEG-COOH@3-MA, (g) PHNPs@DPA-S-S-PEG-BSA-MA@3-MA respectively. To confirm the successful preparation of surface modified PHNPs, FITR spectra were measured as shown in Fig. S5. The infrared spectrum of the synthesized PHNPs was a strong and broad band centered on 3400 cm^{-1}, indicating the chemical reaction of oleic acid and oleylamine on iron oxide nanoparticles. The peaks at 2920 cm^{-1} and 2850 cm^{-1} were caused by symmetric and asymmetric CH_2 stretching modes, respectively (a). After surface modified by DPA of PHNPs, at 1640 cm^{-1}, the contraction vibration peak of dopamine

amino group appeared, indicating that DPA was successfully modified on the surface of PHNPs (b). The contraction vibration peak of N_3 appeared around 2100 cm^{-1}. The frequencies of 1659 cm^{-1} and 1545 cm^{-1} were located in the C=O tensile band (amide I) and the N-H bending band (amide II), respectively (c), indicating that N_3-PEG-COOH was successfully modified on the surface of PHNPs @DPA through amide reaction. The carboxyl group was symmetrically or asymmetrically stretched at 1700 cm^{-1} (d), indicating that the surface carboxylation of PHNPs was successfully achieved by clicking the reaction. To confirm that 3-MA could be loaded into PHNPs, and have no effect on the carboxyl on the surface of PHNPs. The FITR of 3-MA (e) and PHNPs@DPA-S-S-PEG-COOH@3-MA (f) was measured. The carboxyl group was symmetrically or asymmetrically stretched at 1692 cm^{-1} (f). The carboxyl peaks around 1700 cm^{-1} disappeared, and the amino peaks around 1659 cm^{-1} and 1545 cm^{-1} were strengthened and widened, indicating that PHNPs@DPA-S-S-PEG-BSA-MA@3-MA was successfully synthesized (e).[S1]

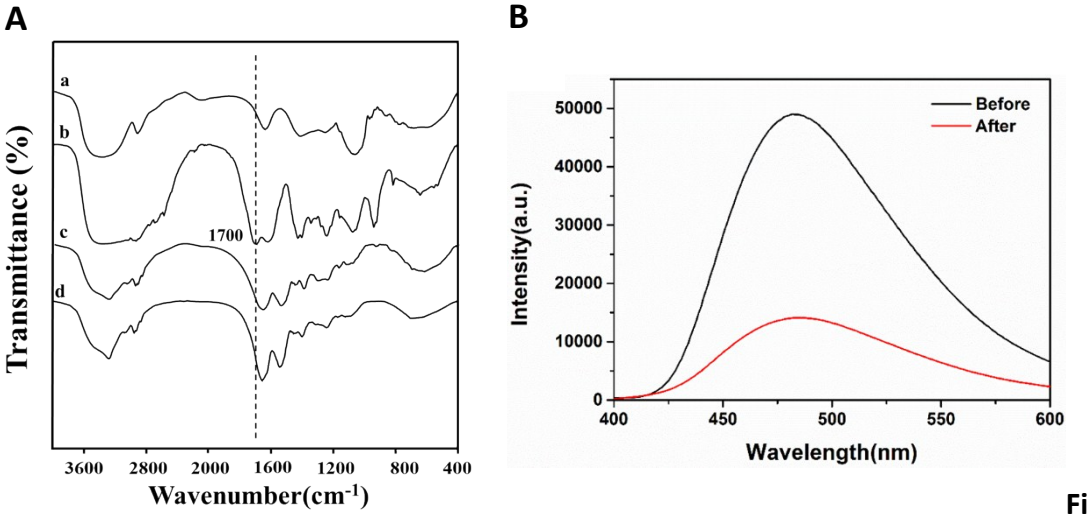

Fig. S6. A. FTIR spectra of MA (a), MA-COOH (b), BSA (c), BSA-MA (d). B. Fluorescent amine of BSA and BSA-MA, respectively.

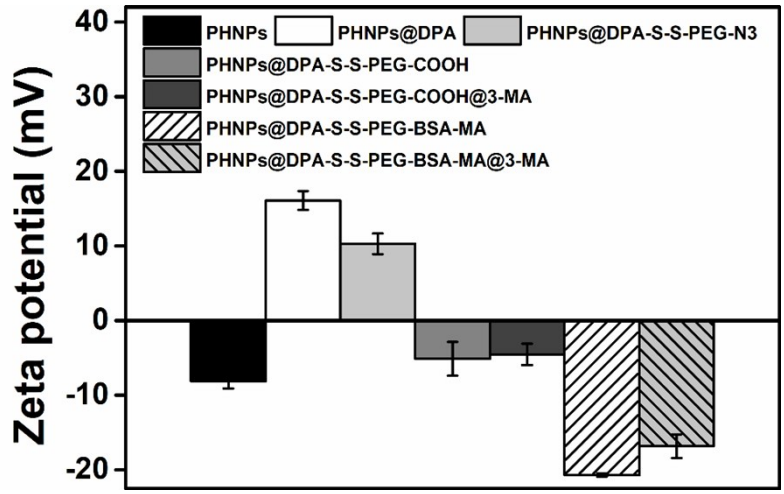

Fig. S7. Zeta potential change of PHNPs, PHNPs@DPA, PHNPs@DPA-S-S-PEG-N_3, PHNPs@DPA-S-S-PEG-COOH, PHNPs@DPA-S-S-PEG-COOH@3-MA, PHNPs@DPA-S-S-PEG-BSA-MA and PHNPs@DPA-S-S-PEG-BSA-MA@3-MA, respectively (n=6).

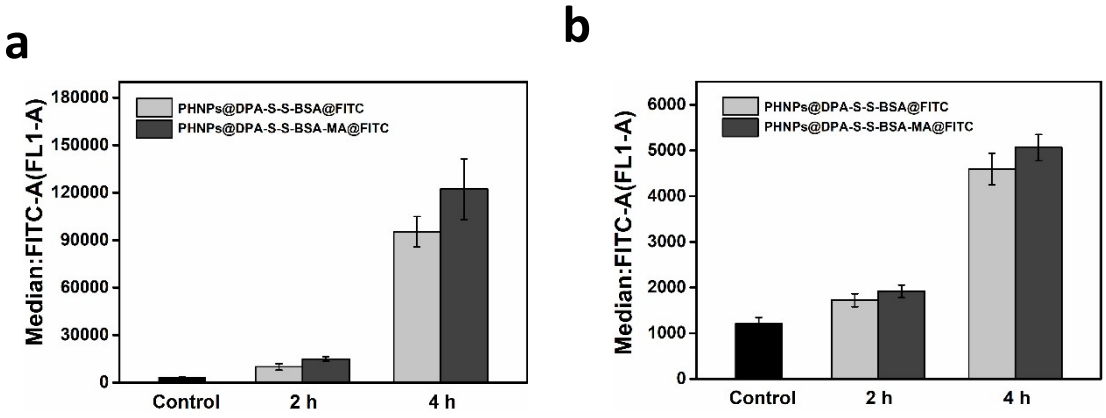

Fig. S8. The median of MDA-MB-231 and HUVEC cells for phagocytosis of PHNPs@DPA-S-S-BSA@FITC and PHNPs@DPA-S-S-BSA-MA@FITC after incubation for 2 and 4 h. It was detected by Flow cytometry.

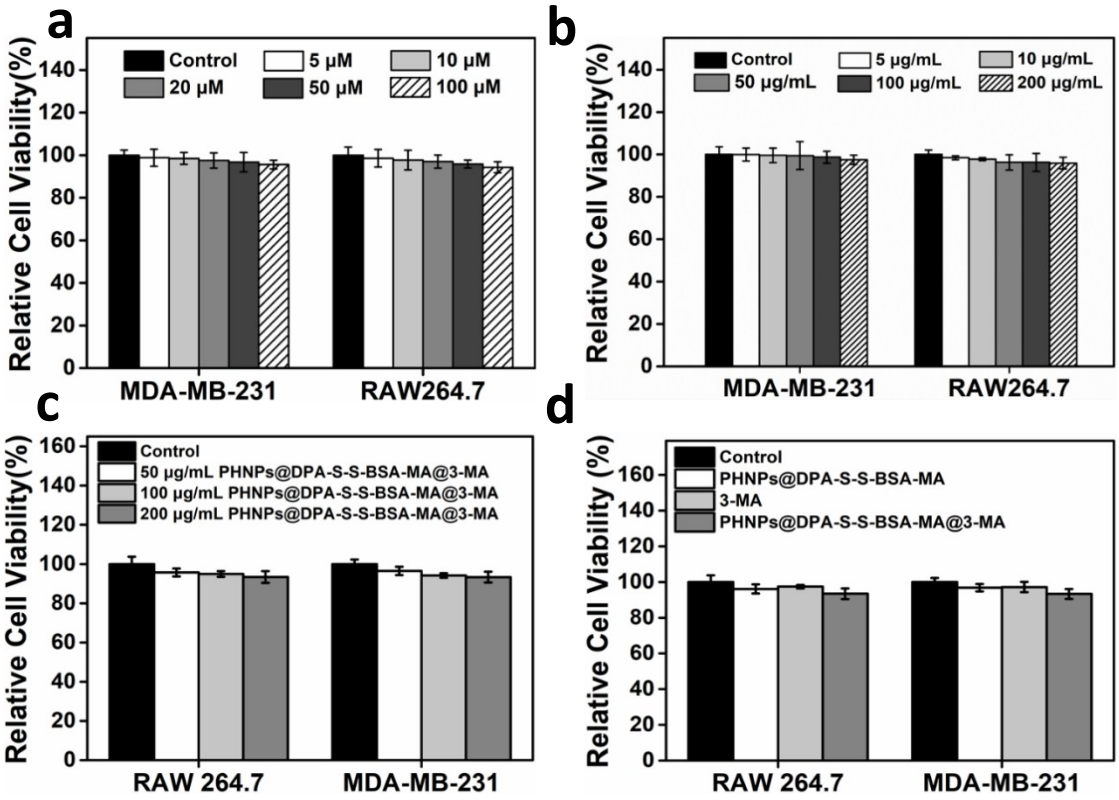

Fig. S9. Cell viability assay of RAW 264.7 cells and MDA-MB-231 cells treated with various concentrations of 3-MA (a), PHNPs@DPA-S-S-BSA-MA (b) and PHNPs@DPA-S-S-BSA-MA@3-MA (c) for 24 h. (d) Cell viability assay of RAW 264.7 cells and MDA-MB-231 cells treated with PHNPs@DPA-S-S-BSA-MA (200 μg/mL), 3-MA (66.9 μM), and PHNPs@DPA-S-S-BSA-MA@3-MA(200 μg/mL), respectively (n=6).

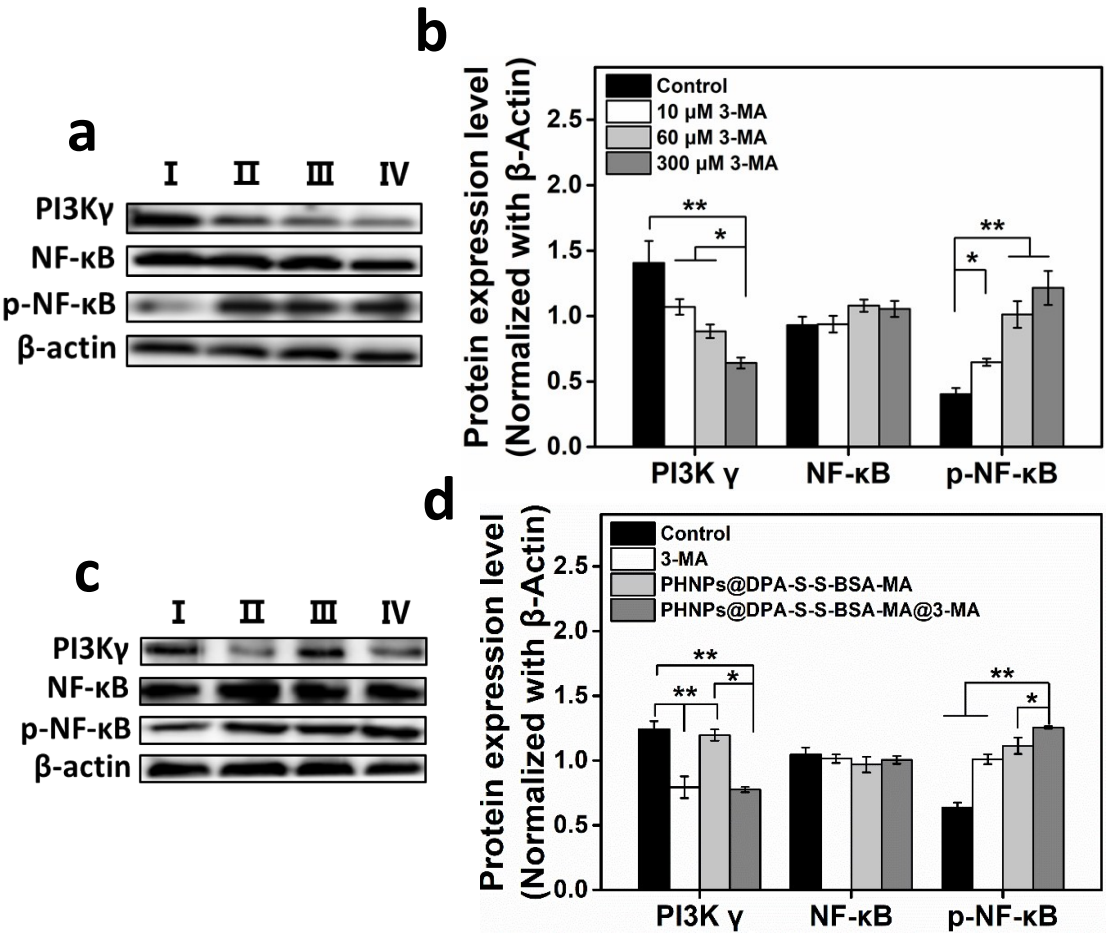

Fig. S10. (a) Western blotting assay to investigate that various concentration of 3-MA inhibited P13K γ expression and activated NF-κBp65 expression in MDA-MB-231 cells. (b) Quantitative analysis of PI3K γ, NF-κBp65 and p-NF-κBp65 expression in MDA-MB-231 cells under various concentrations of 3-MA. (c) Western blotting of PI3K γ, NF-κBp65 and p-NF-κBp65 expression in MDA-MA-231 cells under different treatments: control(Ⅰ), 66.9 μM of 3-MA (Ⅱ), 200 μg/mL of PHNPs@DPA-S-S-BSA-MA (Ⅲ) and 200 μg/mL of PHNPs@DPA-S-S-BSA-MA@3-MA (Ⅳ). (d) Quantitative analysis of PI3K γ, NF-κBp65 and p-NF-κBp65, expression in the MDA-MB-231 cells under different treatments. Error bars are standard error of the mean (n=3), *$p < 0.05$, **$p < 0.01$.

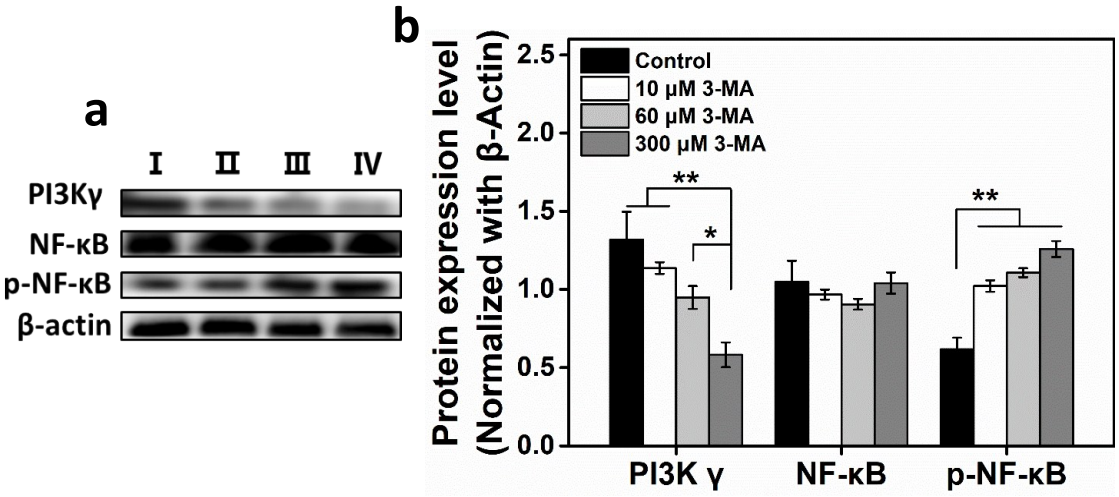

Fig. S11. (a) Western blotting was detected to investigate that various concentration of 3-MA inhibit the expression of P13K γ and activated the expression of NF-κBp65 in RAW 264.7 cells. (b) Quantitative analysis of PI3K γ, NF-κBp65 and p-NF-κBp65, expression in the RAW 264.7 cells under various concentration of 3-MA. Error bars are standard error of the mean (n=3), *$p < 0.05$, **$p < 0.01$.[S2]

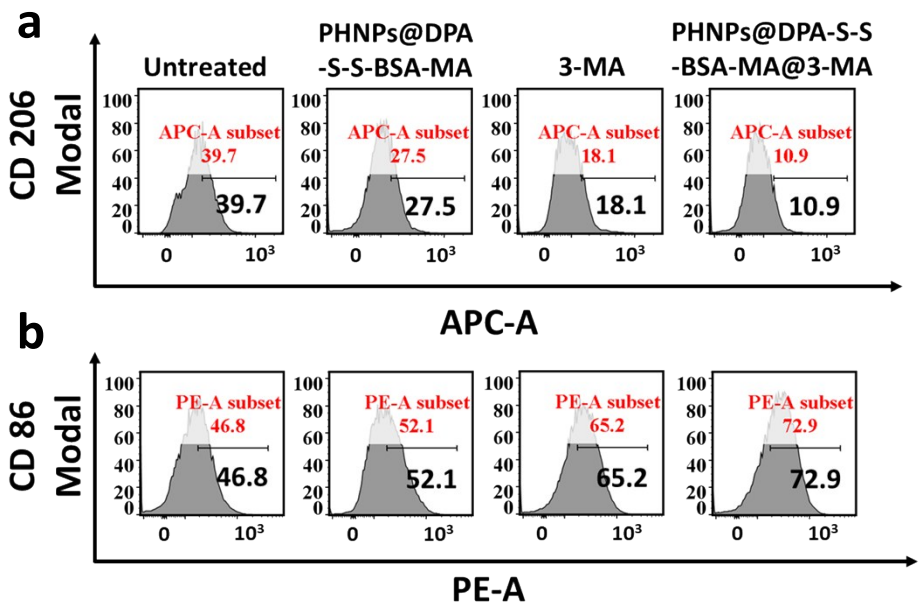

Fig. S12. Flow cytometry analysis the expression of CD 206 (a) and CD 86 (b) in RAW 264.7 cells.

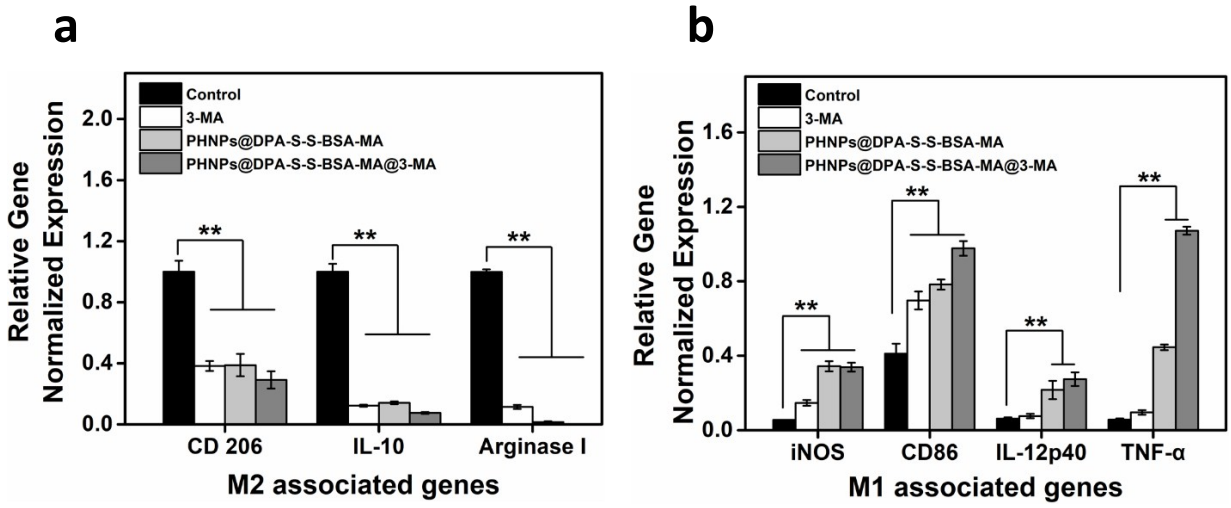

Fig. S13. The qRT-PCR analysed the gene expression of RAW 264.7 cells: a, M2 associated genes and b, M1 associated genes (n=3).

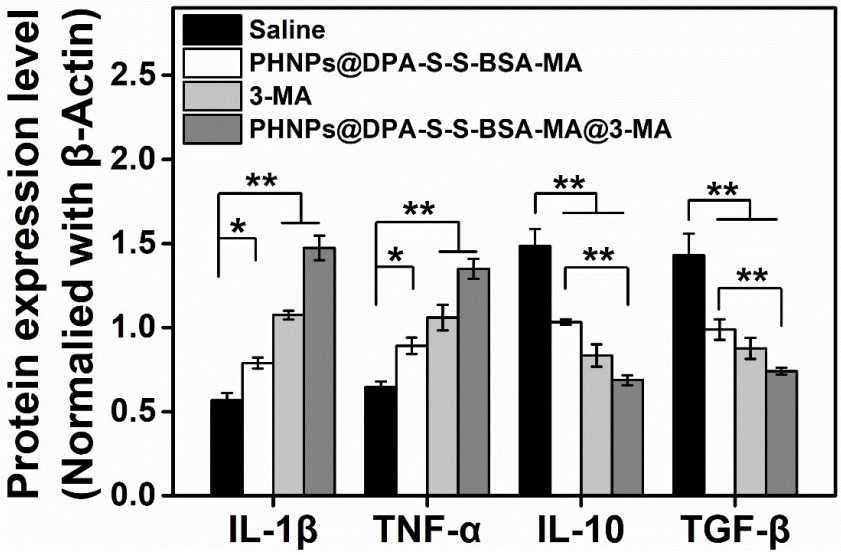

Fig. S14. Quantitative analysis of IL-1β, TNF-α, IL-10 and TGF-β expression in the tumor sections under different treatments for 21 days. Error bars are standard error of the mean (n=3), *$p < 0.05$, **$p < 0.01$.

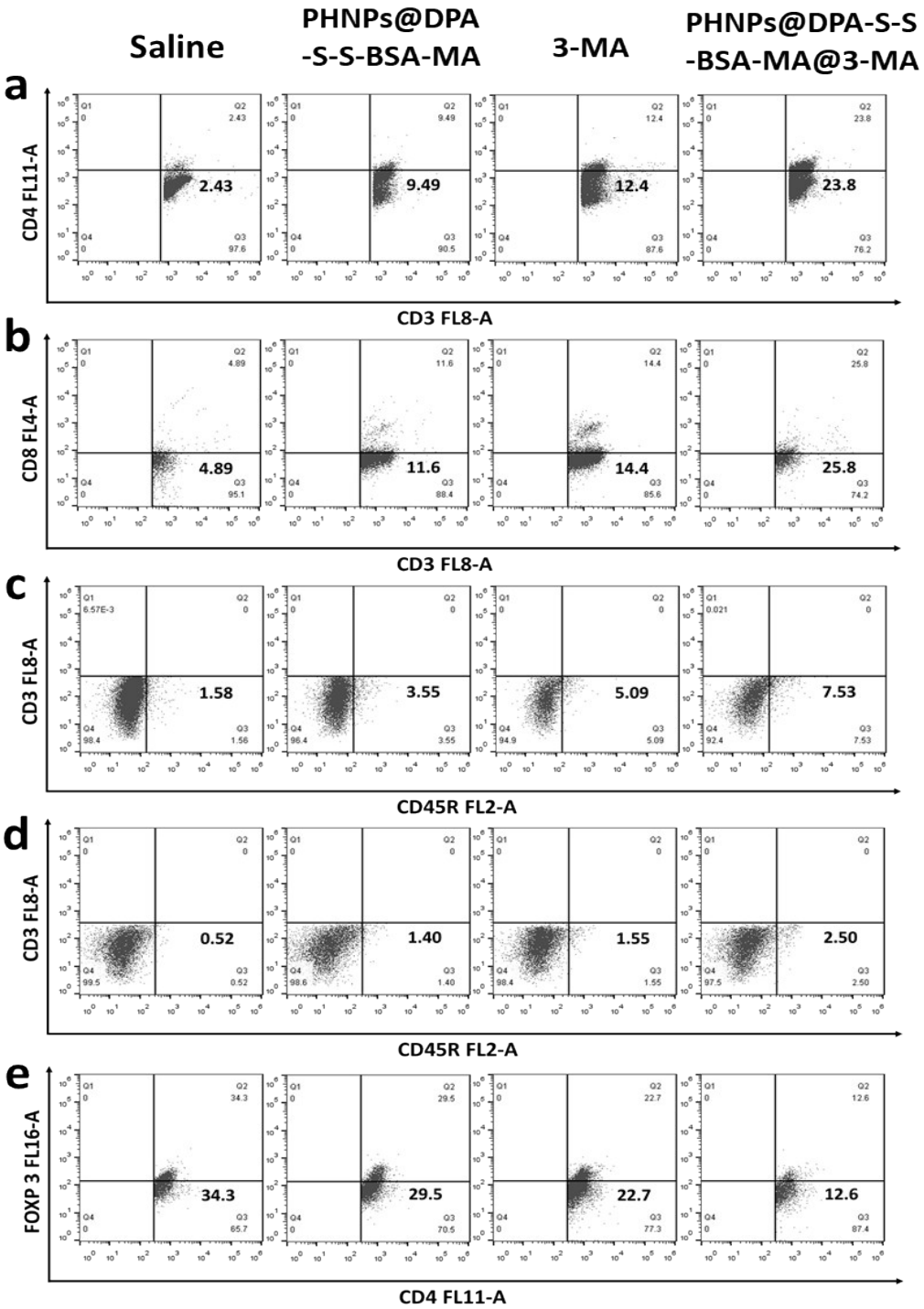

Fig. S15. Flow cytometry detection of the tumor-infiltrating CD 4 cells ($CD4^+CD3^+CD45^+$), CD8 cells ($CD8^+CD3^+CD45^+$), B cells ($CD45R^+CD45^+$), NK cells ($CD49B^+CD45^+$) and Treg cells ($FoXP3^+CD4^+CD25^+$) in MDA-MB-231 tumor-bearing Balb/c mice under different treatments for 21 days.

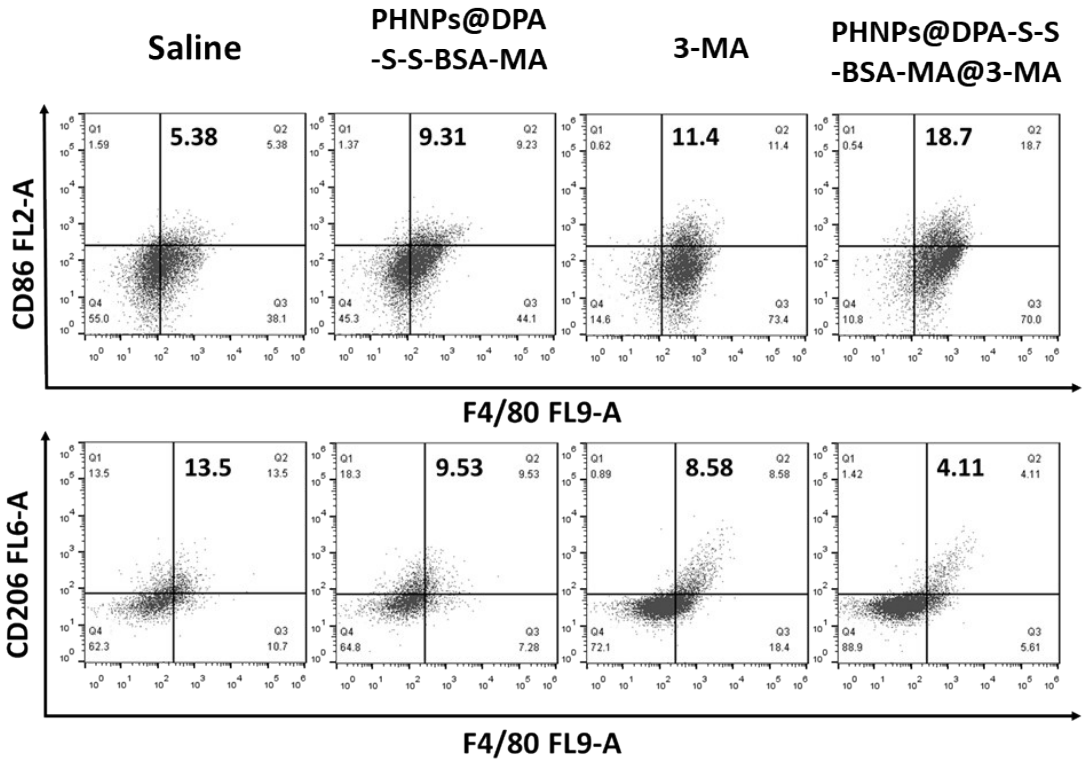

Fig. S16. Flow cytometry detection of the tumor-associated macrophages M2 phenotype ($CD206^+F4/80^+CD11b^+$) and M1 phenotype ($CD86^+F4/80^+CD11b^+$) in MDA-MB-231 tumor-bearing Balb/c mice under different treatments for 21 days.[S3]

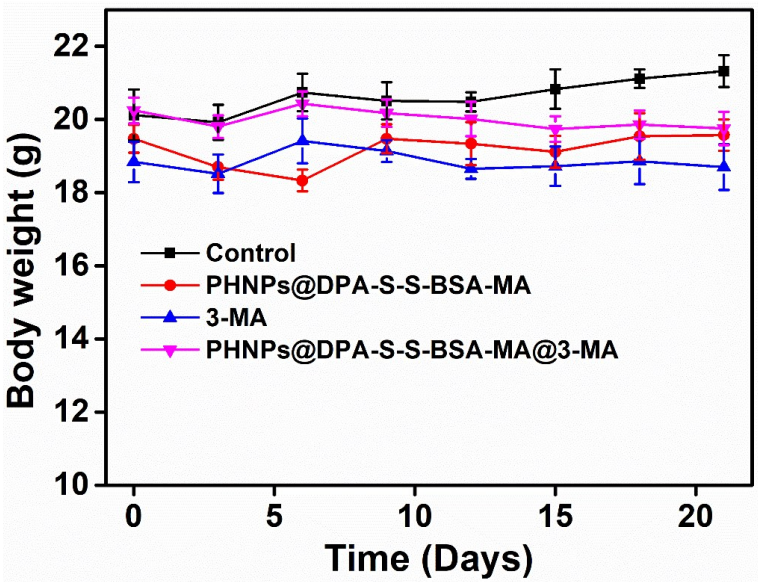

Fig. S17. The curve of body weight change of bearing MDA-MB-231 tumors mice after different treatments. Error bars are standard error of the mean (n=6), *$p < 0.05$, **$p < 0.01$.

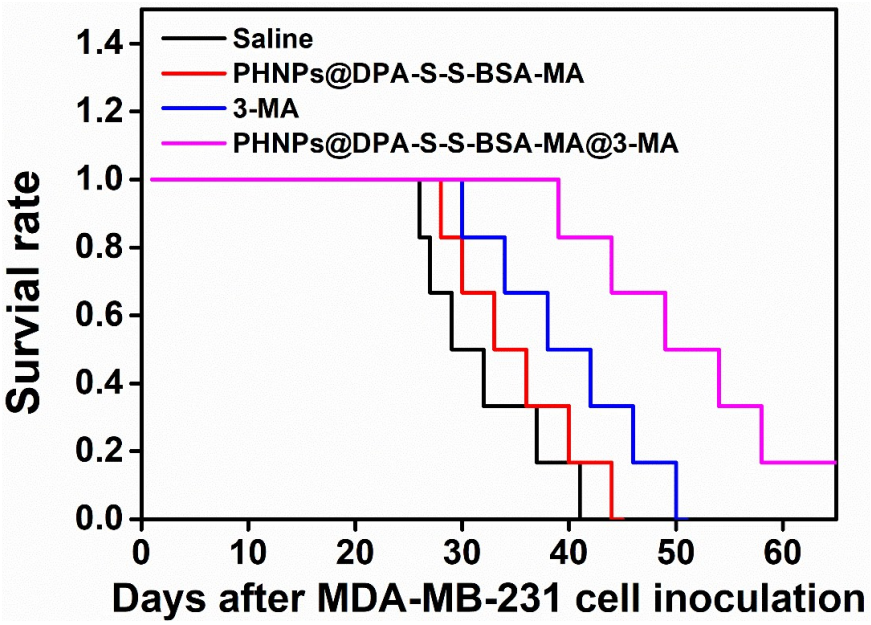

Fig. S18. Mice survival rate after different treatments.

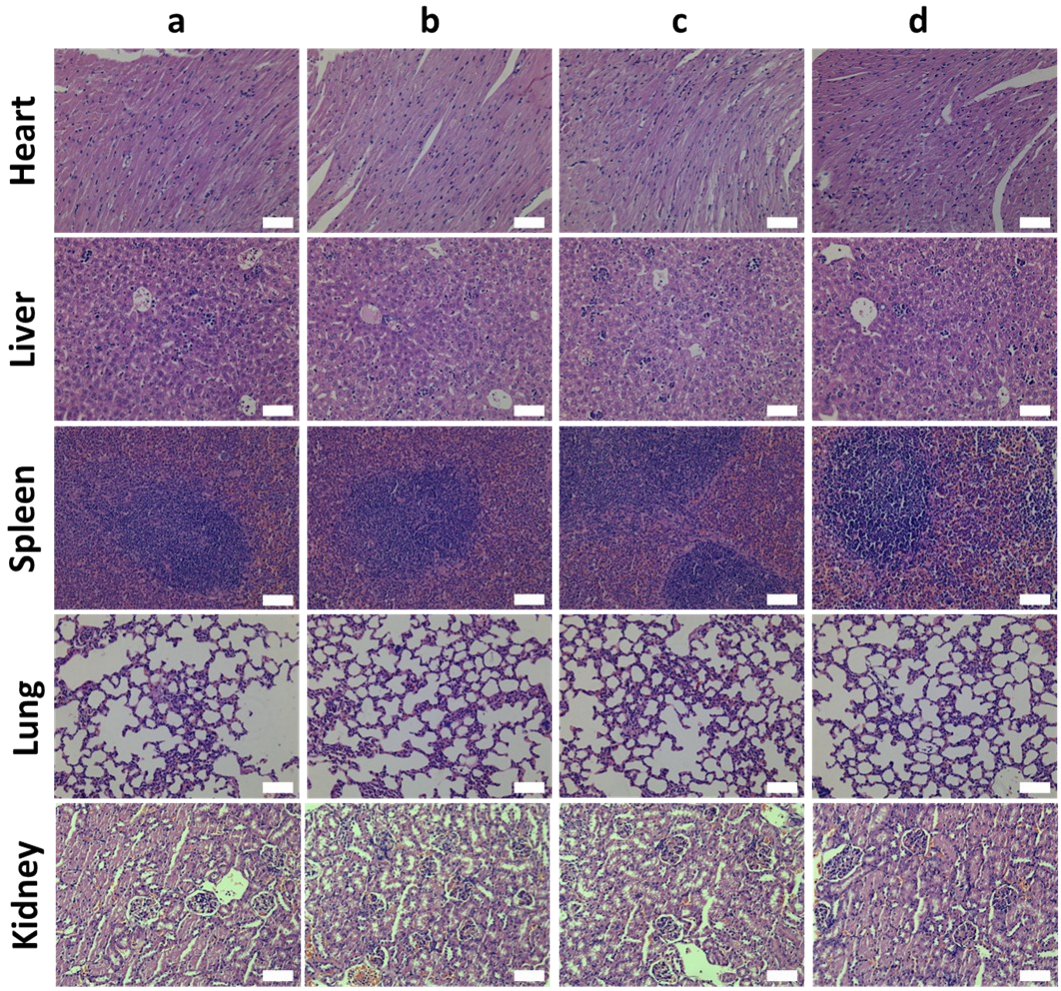

Fig. S19. Images of H&E analysis of major tissues of MDA-MB-231 tumor-bearing Balb/c mice after administration with various treatments for 21 days (a: Saline; b:PHNPs@DPA-S-S-BSA-MA; c:3-MA; d: PHNPs@DPA-S-S-BSA-MA@3-MA). Scale bar: 50 μm.

Table S1. Primers used for qRT-PCR (Mus musculus) in this study.

Genes	Primers
iNOS	5’- GTTCTCAGCCCAACAATACAAGA-3’
	5’- GTGGACGGGTCGATGTCAC-3’
CD86	5’- TCAATGGGACTGCATATCTGCC-3’
	5’- GCCAAAATACTACCAGCTCACT-3’
IL-12p40	5’- ATGGAGTCATAGGCTCTGGAAA-3’
	5’- CCGGAGTAATTTGGTGCTTCAC-3’
Arginase I	5’- TGTCCCTAATGACAGCTCCTT-3’
	5’- GCATCCACCCAAATGACACAT-3’
CD206	5’- AGGCTGATTACGAGCAGTGG-3’
	5’- CCATCACTCCAGGTGAACCC-3’
TGF-β	5’-CTAAGGCTCGCCAGTCCCC-3’
	5’-TGCGTTGTTGCGGTCCAC-3’
IL-10	5’-GCATGGCCCAGAAATCAAGG-3’
	5’-GAGAAATCGATGACAGCGCC-3’
TNF-α	5’- CCATCACTCCAGGTGAACCC-3’
	5’- CGATCACCCCGAAGTTCAGTAG-3’
β-actin	5’- GGAGATTACTGCCCTGGCTCCTA-3’
	5’- GACTCATCGTACTCCTGCTTGCTG-3’

Table S2. Primers used for qRT-PCR (Homo sapiens) in this study.

Genes	Primers
iNOS	5’- TCATCCGCTATGCTGGCTAC-3’
	5’- CCCGAAACCACTCGTATTTGG-3’
CD86	5’- CTGCTCATCTATACACGGTTACC-3’
	5’- GGAAACGTCGTACAGTTCTGTG-3’
IL-12p40	5’- TATCTTTCTTTTCTCTCTTGCTCTT-3’
	5’- CATCAGGGACATCATCAA-3’
Arginase I	5’- TGGACAGACTAGGAATTGGCA-3’
	5’- CCAGTCCGTCAACATCAAAACT-3’
CD206	5’- TCCGGGTGCTGTTCTCCTA-3’
	5’- CCAGTCTGTTTTTGATGGCACT-3’
IL-10	5’- TCAAGGCGCATGTGAACTCC-3’
	5’- GATGTCAAACTCACTCATGGCT-3’
TNF-α	5’- CCTCTCTCTAATCAGCCCTCTG-3’
	5’- GAGGACCTGGGAGTAGATGAG-3’
β-actin	5’- CATGTACGTTGCTATCCAGGC-3’
	5’- CTCCTTAATGTCACGCACGAT-3’

References.

[S1] Z. Luo, K. Cai, Y. Hu, J. Li, X. Ding, B. Zhang, D. Xu, W. Yang and P. Liu, *Adv. Mater.*, 2012, **24**, 431-435.

[S2] M.M. Kaneda, K.S. Messer, N. Ralainirina, H. Li, C.J. Leem, S. Gorjestani, G. Woo, A.V. Nguyen, C.C. Figueiredo, P. Foubert, M.C. Schmid, M. Pink, D.G. Winkler, M. Rausch, V.J. Palombella, J. Kutok, K. McGovern, K.A. Frazer, X. Wu, M. Karin, R. Sasik, E.E. Cohen and J.A. Varner, *Nature,* 2016, **539**, 437-447.

[S3] G.-T. Yu, L. Rao, H. Wu, L.-L. Yang, L.-L. Bu, W.-W. Deng, L. Wu, X. Nan, W. F. Zhang, X.-Z. Zhao, W. Liu and Z.-J. Sun, Adv. Funct. Mater., 2018, **28**, 1801389.